Aalborg Universitet

Message-Passing Receivers for Single Carrier Systems with Frequency-Domain Equalization

Zhang, Chuanzong; Manchón, Carles Navarro; Wang, Zhongyong; Fleury, Bernard Henri

Message-Passing Receivers for Single Carrier Systems with Frequency-Domain Equalization

Chuanzong Zhang, Carles Navarro Manchón, Zhongyong Wang, and Bernard Henri Fleury, *Senior Member, IEEE*

Abstract—In this letter, we design iterative receiver algorithms for joint frequency-domain equalization and decoding in a single carrier system assuming perfect channel state information. Based on an approximate inference framework that combines belief propagation (BP) and the mean field (MF) approximation, we propose two receiver algorithms with, respectively, parallel and sequential message-passing schedules in the MF part. A recently proposed receiver based on generalized approximate message passing (GAMP) is used as a benchmarking reference. The simulation results show that the BP-MF receiver with sequential passing of messages achieves the best BER performance at the expense of higher computational complexity compared to that of the GAMP receiver. The parallel BP-MF receiver has complexity similar to that of GAMP, but its low convergence rate yields poor performance, especially under high signal-to-noise ratio conditions.

Index Terms—Iterative receiver, message-passing, SC-FDE.

I. INTRODUCTION

SINGLE carrier system with frequency domain equalization (SC-FDE) technique is an attractive technology for wireless communications due to its ability to cope with the temporal dispersion introduced by multipath channels. It has the performance, efficiency and low complexity advantages over its orthogonal frequency division multiplexing (OFDM) counterpart, while being less sensitive to power amplifier nonlinearities and carrier frequency offsets, in addition to exhibiting a lower peak-to-average transmitted power ratio [1]. For these reasons, SC-FDE has been selected as the access scheme for the uplink of the 3GPP long term evolution (LTE) and LTE advanced standards [2].

Belief propagation (BP) on factor graphs, also known as sum-product algorithm [3], is a message-passing inference technique that has been widely used in the design of iterative wireless receivers. Its remarkable performance, especially when applied to discrete probabilistic models, justifies its popularity. However, its complexity may become intractable in certain application contexts, e.g. when the probabilistic model includes both discrete and continuous random variables.

As an alternative to BP, variational methods based on the mean field (MF) approximation [4] have been initially used in quantum and statistical physics. The MF approximation has also been formulated as a message passing algorithm, referred to as variational message passing (VMP) algorithm [5]. It has primarily been used on continuous probabilistic conjugate-exponential models. Recently, a method that combines BP and MF [6] as a unified message passing framework on a same factor graph has been proposed, which keeps the virtues of BP and MF but avoids their respective drawbacks. The BP-MF method was applied to joint channel estimation and decoding in MIMO-OFDM systems [7].

As an alternative approach to deal with the high complexity problem of BP, researchers are also pursuing approximate BP methods. The approximate message passing (AMP) approach was derived from BP by approximating some messages to be Gaussian by invoking the central limit theorem and Taylor expansions, and was initially proposed for compressed sensing [8]. Recently, Rangan extended AMP to the general estimation problem with linear mixing and developed the so-called the generalized approximated message-passing (GAMP) algorithm [9]. GAMP operates as a parallel message passing scheme. It has been previously used for turbo sparse channel estimation and frequency-domain equalization in OFDM systems [10], turbo equalization in SC-FDE systems [11], and iterative channel estimation and detection in OFDM systems impaired by impulsive noise [12].

In this letter, based on the combined inference technique presented in [6], we develop a parallel and a sequential message-passing receiver for a SC-FDE system and compare its performance with an analogous iterative receiver, inspired by [11], implementing GAMP in the equalization part.

Notation: Boldface lowercase and uppercase letters denote vectors and matrices, respectively, while superscripts $(\cdot)^*$, $(\cdot)^{\mathrm{T}}$ and $(\cdot)^{\mathrm{H}}$ represent conjugation, transposition and Hermitian transposition, respectively. The expectation operator with respect to a density $g(x)$ is expressed by $\langle f(x) \rangle_{g(x)} = \int f(x)g(x)dx / \int g(x')dx'$, while $\mathrm{var}[x]_{g(x)} = \langle |x|^2 \rangle_{g(x)} - |\langle x \rangle_{g(x)}|^2$ represents the variance. The pdf of a complex Gaussian distribution with mean μ and variance ν is represented by $\mathcal{CN}(x; \mu, \nu)$. The relation $f(x) = cg(x)$ for some positive constant c is written as $f(x) \propto g(x)$. We use $\| \cdot \|$ to stand for Euclidian norm. The $N \times N$ normalized discrete Fourier matrix is denoted by $\boldsymbol{F}$, with entries $F_{ai} = 1/\sqrt{N}e^{-j2\pi(a-1)(i-1)/N}$.
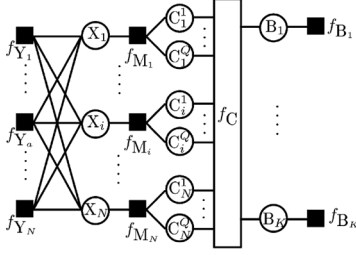
Fig. 1. Factor graph representing the probabilistic model in (2).

II. SYSTEM MODEL

The finite sequence of information bits $\boldsymbol{b} = [b_1, \ldots, b_K]^{\mathrm{T}}$ of an SC-FDE block is encoded and interleaved by using a rate R channel code and a random interleaver, yielding the codeword vector $\boldsymbol{c} = [\boldsymbol{c}_1^{\mathrm{T}}, \ldots, \boldsymbol{c}_N^{\mathrm{T}}]^{\mathrm{T}}$, where the ith sub-vector is $\boldsymbol{c}_i = [c_i^1, \ldots, c_i^Q]^{\mathrm{T}}$ with Q denoting the modulation order. The codeword $\boldsymbol{c}$ is complex modulated, resulting in the vector of data symbols $\boldsymbol{x} = [x_1, \ldots, x_N]^{\mathrm{T}}$, which is transmitted over the wireless channel after the addition of a cyclic prefix (CP). At the receiver end, the CP is removed and the received signal is Fourier transformed, yielding

$$\boldsymbol{y} = \boldsymbol{H}\boldsymbol{z} + \boldsymbol{w} = \boldsymbol{H}\boldsymbol{F}\boldsymbol{x} + \boldsymbol{w}, \tag{1}$$

where $\boldsymbol{H} = \mathrm{diag}(\boldsymbol{h})$ with $\boldsymbol{h} = [h_1, h_2, \ldots, h_N]^{\mathrm{T}}$ representing the vector of frequency-domain channel weights, $\boldsymbol{z} = \boldsymbol{F}\boldsymbol{x}$ is a vector containing the equivalent frequency-domain data symbols and $\boldsymbol{w}$ is a complex additive white Gaussian noise vector with covariance matrix $\lambda^{-1}\boldsymbol{I}$.

A. Probabilistic Representation and Factor Graph

Based on (1), we can factorize the joint pdf of all unknown random variables conditioned on the observation $\boldsymbol{y}$ as

$$p(\boldsymbol{x}, \boldsymbol{c}, \boldsymbol{b}|\boldsymbol{y})$$
$$\propto \prod_{a=1}^{N} f_{\mathrm{Y}_a}(y_a, \boldsymbol{x}) \prod_{i=1}^{N} f_{\mathrm{M}_i}(x_i, \boldsymbol{c}_i) f_{\mathrm{C}}(\boldsymbol{c}, \boldsymbol{b}) \prod_{k=1}^{K} f_{\mathrm{B}_k}(b_k) \tag{2}$$

where $f_{\mathrm{Y}_a}(y_a, \boldsymbol{x}) \triangleq p(y_a|\boldsymbol{x}) = \mathcal{CN}(y_a; h_a \boldsymbol{F}_a \boldsymbol{x}, \lambda^{-1})$ with $\boldsymbol{F}_a$ being the ath row of $\boldsymbol{F}$ and h_a being the ath entry of $\boldsymbol{h}$, $f_{\mathrm{M}_i}(x_i, \boldsymbol{c}_i)$ and $f_{\mathrm{C}}(\boldsymbol{c}, \boldsymbol{b})$ stand for the modulation and coding constraints, and $f_{\mathrm{B}_k}(b_k) \triangleq p(b_k)$ is the prior of the kth information bit. In (2), we have used the fact that, given $\boldsymbol{x}$, $\boldsymbol{y}$ is conditionally independent of $\boldsymbol{c}$ and $\boldsymbol{b}$. The factor graph [3] shown on Fig. 1 represents the above factorization.

III. COMBINED BP AND MF FRAMEWORK

In this section, we derive the messages passed on the factor graph shown in Fig. 1 by using the BP-MF message updating rules [6] and discuss their scheduling.

We group the factor nodes in two disjoint subsets, a BP part for demodulation and decoding, and an MF part for equalization,

$$\mathcal{A}_{\mathrm{MF}} = \{f_{\mathrm{Y}_a}; a \in [1:N]\}$$
$$\mathcal{A}_{\mathrm{BP}} = \{f_{\mathrm{M}_i}; i \in [1:N]\} \cup \{f_{\mathrm{C}}\} \cup \{f_{\mathrm{B}_k}; k \in [1:K]\},$$

where $\mathcal{A}_{\mathrm{MF}}$ and $\mathcal{A}_{\mathrm{BP}}$ denote the sets of factor nodes in the MF and BP parts, respectively. For factor nodes in the BP part, we calculate the messages to neighboring variable nodes using the sum-product rule, and send extrinsic messages. For factor nodes

in the MF part, messages to neighboring variable nodes are computed by the VMP rule, and beliefs are passed.

Due to the factor nodes $\{f_{\mathrm{M}_i}\}$ being in the BP part, the extrinsic messages passed from X_i to f_{M_i}, $i = 1, \ldots, N$, read

$$n_{\mathrm{X}_i \to f_{\mathrm{M}_i}}(x_i) \propto \prod_{a=1}^{N} m_{f_{\mathrm{Y}_a} \to \mathrm{X}_i}(x_i)$$
$$\triangleq \mathcal{CN}(x_i; \mu_{\mathrm{X}_i \to f_{\mathrm{M}_i}}, \nu_{\mathrm{X}_i \to f_{\mathrm{M}_i}}). \tag{3}$$

Messages $\{m_{f_{\mathrm{M}_i} \to \mathrm{X}_i}(x_i)\}$, yielded by the sum-product rule, come from the soft demodulation part. Messages from X_i to f_{Y_a} in the MF part correspond, for all a, to the belief $b(x_i)$, which is computed by collecting the messages from all neighbors of X_i, i.e.

$$b(x_i) = n_{\mathrm{X}_i \to f_{\mathrm{Y}_a}}(x_i) \propto \prod_{a=1}^{N} m_{f_{\mathrm{Y}_a} \to \mathrm{X}_i}(x_i) m_{f_{\mathrm{M}_i} \to \mathrm{X}_i}(x_i)$$
$$\propto n_{\mathrm{X}_i \to f_{\mathrm{M}_i}}(x_i) m_{f_{\mathrm{M}_i} \to \mathrm{X}_i}(x_i), \tag{4}$$
$$\mu_{\mathrm{X}_i \to \mathrm{Y}} \triangleq \langle x_i \rangle_{b(x_i)}, \tag{5}$$
$$\nu_{\mathrm{X}_i \to \mathrm{Y}} \triangleq \mathrm{var}[x_i]_{b(x_i)}. \tag{6}$$

We group the parameters $\{\mu_{\mathrm{X}_i \to \mathrm{Y}}\}$ into the vector $\boldsymbol{\mu}_{\mathrm{X} \to \mathrm{Y}} = [\mu_{\mathrm{X}_1 \to \mathrm{Y}}, \mu_{\mathrm{X}_2 \to \mathrm{Y}}, \ldots, \mu_{\mathrm{X}_N \to \mathrm{Y}}]^{\mathrm{T}}$.

Using the VMP rule and the messages $\{n_{\mathrm{X}_i \to f_{\mathrm{Y}_a}}(x_i)\}$, the messages from f_{Y_a} to X_i are obtained as

$$m_{f_{\mathrm{Y}_a} \to \mathrm{X}_i}(x_i) \propto \exp\left\{ \langle \log f_{\mathrm{Y}_a}(y_a, \boldsymbol{x}) \rangle_{\prod_{j \neq i} b(x_j)} \right\}$$
$$\propto \mathcal{CN}\left(x_i; \mu_{f_{\mathrm{Y}_a} \to \mathrm{X}_i}, \nu_{f_{\mathrm{Y}_a} \to \mathrm{X}_i}\right), \tag{7}$$

where $\mu_{f_{\mathrm{Y}_a} \to \mathrm{X}_i} \triangleq F_{ai}^* h_a^*(y_a - h_a \boldsymbol{F}_a \boldsymbol{\mu}_{\mathrm{X}_{\bar{i}} \to \mathrm{Y}})/(F_{ai}^* h_a^* h_a F_{ai})$, $\boldsymbol{\mu}_{\mathrm{X}_{\bar{i}} \to \mathrm{Y}}$ is equal to $\boldsymbol{\mu}_{\mathrm{X} \to \mathrm{Y}}$ with its ith entry replaced by 0, and $\nu_{f_{\mathrm{Y}_a} \to \mathrm{X}_i} \triangleq 1/(\lambda F_{ai}^* h_a^* h_a F_{ai})$.

Substituting (7) into (3), we obtain

$$\mu_{\mathrm{X}_i \to f_{\mathrm{M}_i}} = \frac{1}{C} \boldsymbol{F}_i^{\mathrm{H}} \boldsymbol{H}^{\mathrm{H}}\left(\boldsymbol{y} - \boldsymbol{H}\boldsymbol{F}\boldsymbol{\mu}_{\mathrm{X}_{\bar{i}} \to \mathrm{Y}}\right) \tag{8}$$
$$\nu_{\mathrm{X}_i \to f_{\mathrm{M}_i}} = (\lambda C)^{-1} \tag{9}$$

where $\boldsymbol{F}_i$ is the ith column of $\boldsymbol{F}$, and $C \triangleq \boldsymbol{F}_i^{\mathrm{H}} \boldsymbol{H}^{\mathrm{H}} \boldsymbol{H} \boldsymbol{F}_i = \frac{\|\boldsymbol{h}\|^2}{N}$.

The factor graph in Fig. 1 is very densely connected, especially in the MF part. Hence, there is a multitude of different options for scheduling the messages. In this letter, the standard message-passing schedule is chosen for the BP part. Messages are passed from the modulation nodes to the coding node in parallel, followed by a round of decoding using the forward-backward (BCJR) algorithm [3], and the outcome messages are passed to the modulation nodes simultaneously. For the MF part, we propose two kinds of scheduling, a parallel schedule and a sequential schedule, which are described next.

A. The Parallel Schedule

The messages $\{n_{\mathrm{X}_i \to f_{\mathrm{Y}_a}}^t(x_i)\}$ (beliefs) from variable nodes $\{\mathrm{X}_i\}$ to factor nodes $\{f_{\mathrm{Y}_a}\}$ are computed from (3) and (4). The superscript t denotes the iteration index. All the messages $\{m_{f_{\mathrm{Y}_a} \to \mathrm{X}_i}^t(x_i)\}$ from factor nodes $\{f_{\mathrm{Y}_a}\}$ to variable nodes $\{\mathrm{X}_i\}$ are simultaneously computed using (7). The aforementioned process is carried out twice per iteration. Subsequently, messages $\{n_{\mathrm{X}_i \to f_{\mathrm{M}_i}}^t(x_i)\}$ from $\{\mathrm{X}_i\}$ to $\{f_{\mathrm{M}_i}\}$ are computed using (8) and (9) and passed on to the BP part. The above procedure is summarized in **Algorithm 1**.

Algorithm 1 BP-MF with Parallel Scheduling

1:   **for all** i: initialize $m^0_{f_{M_i} \to X_i}(x_i), \mu^0_{X_i \to f_{M_i}}, \nu^0_{X_i \to f_{M_i}}$.

2:   **for all** i: $\mu^0_{X_i \to Y} \leftarrow \langle x_i \rangle_{\mathcal{CN}(x_i; \mu^0_{X_i \to f_{M_i}}, \nu^0_{X_i \to f_{M_i}}) m^0_{f_{M_i} \to X_i}(x_i)}$

3:   **for** $t = 1 \to$ Iteration **do**

4:       $\boldsymbol{\mu}^t_Z \leftarrow \boldsymbol{y} - \boldsymbol{HF}\boldsymbol{\mu}^{t-1}_{X \to Y}$

5:       **for all** i: $\mu^t_{X_i \to f_{M_i}} \leftarrow \frac{1}{C}\boldsymbol{F}^H_i \boldsymbol{H}^H \boldsymbol{\mu}^t_Z + \mu^t_{X_i \to Y}$

6:       **for all** i: $\nu^t_{X_i \to f_{M_i}} \leftarrow \frac{1}{\lambda C}$

7:       **for all** i: $\mu^t_{X_i \to Y} \leftarrow \langle x_i \rangle_{\mathcal{CN}(x_i; \mu^t_{X_i \to f_{M_i}}, \nu^t_{X_i \to f_{M_i}}) m^{t-1}_{f_{M_i} \to X_i}(x_i)}$

8:       $\boldsymbol{\mu}^t_Z \leftarrow \boldsymbol{y} - \boldsymbol{HF}\boldsymbol{\mu}^t_{X \to Y}$

9:       **for all** i: $\mu^t_{X_i \to f_{M_i}} \leftarrow \frac{1}{C}\boldsymbol{F}^H_i \boldsymbol{H}^H \boldsymbol{\mu}^t_Z + \mu^t_{X_i \to Y}$

10:      **for all** i: $\nu^t_{X_i \to f_{M_i}} \leftarrow \frac{1}{\lambda C}$

11:      **for all** i: $\mathcal{CN}(x_i; \mu^t_{X_i \to f_{M_i}}, \nu^t_{X_i \to f_{M_i}}) \to$ BP part

12:      **for all** i: $m^t_{f_{M_i} \to X_i}(x_i) \leftarrow$ BP part

13:      **for all** i: $\mu^t_{X_i \to Y} \leftarrow \langle x_i \rangle_{\mathcal{CN}(x_i; \mu^t_{X_i \to f_{M_i}}, \nu^t_{X_i \to f_{M_i}}) m^t_{f_{M_i} \to X_i}(x_i)}$

14: **end for** t

B. The Sequential Schedule

Similar to the parallel schedule, the messages $\{n^t_{X_i \to f_{Y_a}}(x_i)\}$ from variable nodes $\{X_i\}$ to factor nodes $\{f_{Y_a}\}$ are computed first. Then, sequentially for each i from 1 to N, the messages $\{m^t_{Y_a \to X_i}(x_i)\}$ are computed using messages $\{n^{t-1}_{X_k \to f_{Y_a}}(x_k); k \in [i+1:N], a \in [1:N]\}$ and $\{n^t_{X_j \to f_{Y_a}}(x_j); j \in [1:i-1], a \in [1:N]\}$. Before calculating messages from factor nodes $\{f_{Y_a}\}$ to variable node X_{i+1}, the messages $\{n^t_{X_i \to f_{Y_a}}(x_i)\}$ are updated using (4). Finally, extrinsic messages $\{n^t_{X_i \to f_{M_i}}(x_i)\}$ are delivered to the BP part. The above procedure is illustrated in **Algorithm 2**.

Algorithm 2 BP-MF with Sequential Scheduling

1:   **for all** i: initialize $m^0_{f_{M_i} \to X_i}(x_i), \mu^0_{X_i \to f_{M_i}}, \nu^0_{X_i \to f_{M_i}}$.

2:   **for all** i: $\mu^0_{X_i \to Y} \leftarrow \langle x_i \rangle_{\mathcal{CN}(x_i; \mu^0_{X_i \to f_{M_i}}, \nu^0_{X_i \to f_{M_i}}) m^0_{f_{M_i} \to X_i}(x_i)}$

3:   **for** $t = 1 \to$ Iteration **do**

4:       $\boldsymbol{\mu}^t_Z \leftarrow \boldsymbol{y} - \boldsymbol{HF}\boldsymbol{\mu}^{t-1}_{X \to Y}$

5:       **for** $i = 1 \to N$ **do**

6:           $\mu^t_{X_i \to f_{M_i}} \leftarrow \frac{1}{C}\boldsymbol{F}^H_i \boldsymbol{H}^H \boldsymbol{\mu}^t_Z + \mu^{t-1}_{X_i \to Y}$

7:           $\nu^t_{X_i \to f_{M_i}} \leftarrow \frac{1}{\lambda C}$

8:           $\mu^t_{X_i \to Y} \leftarrow \langle x_i \rangle_{\mathcal{CN}(x_i; \mu^t_{X_i \to f_{M_i}}, \nu^t_{X_i \to f_{M_i}}) m^{t-1}_{f_{M_i} \to X_i}(x_i)}$

9:           $\boldsymbol{\mu}^t_Z \leftarrow \boldsymbol{\mu}^t_Z + \boldsymbol{HF}_i(\mu^t_{X_i \to Y} - \mu^{t-1}_{X_i \to Y})$

10:      **end for** i

11:      **for all** i: $\mathcal{CN}(x_i; \mu^t_{X_i \to f_{M_i}}, \nu^t_{X_i \to f_{M_i}}) \to$ BP part

12:      **for all** i: $m^t_{f_{M_i} \to X_i}(x_i) \leftarrow$ BP part

13:      **for all** i: $\mu^t_{X_i \to Y} \leftarrow \langle x_i \rangle_{\mathcal{CN}(x_i; \mu^t_{X_i \to f_{M_i}}, \nu^t_{X_i \to f_{M_i}}) m^t_{f_{M_i} \to X_i}(x_i)}$

14: **end for** t

C. Noise Precision Estimation

The above algorithms assume that the noise precision λ is known. However, the BP-MF framework allows for estimating the noise precision if necessary. In this case λ is an unknown variable and the probabilistic model (2) is modified as follows: $p(\boldsymbol{x}, \boldsymbol{c}, \boldsymbol{b}|\boldsymbol{y})$ becomes $p(\boldsymbol{x}, \boldsymbol{c}, \boldsymbol{b}, \lambda|\boldsymbol{y})$, $f_{Y_a}(y_a, \boldsymbol{x})$ is replaced by $f_{Y_a}(y_a, \boldsymbol{x}, \lambda) \triangleq p(y_a|\boldsymbol{x}, \lambda)$ and an additional factor $f_\Lambda(\lambda) \triangleq p(\lambda)$, denoting the prior distribution of λ, is inserted in the factorization. A variable node Λ and a factor node f_Λ are drawn on factor graph Fig. 1 with f_Λ connected to Λ, and Λ also

linked to the factor nodes $\{f_{Y_a}\}$. With the improper prior pdf $p(\lambda) \propto 1/\lambda$, the update for $\hat{\lambda}$ reads [7]

$$\hat{\lambda} = N / \left(\|\boldsymbol{\mu}_Z\|^2 + \|\boldsymbol{h}\|^2 \sum_{i=1}^{N} \nu_{X_i \to Y} \right), \tag{10}$$

where $\nu_{X_i \to Y} = \text{var}[x_i]_{\mathcal{CN}(x_i; \mu_{X_i \to f_{M_i}}, \nu_{X_i \to f_{M_i}}) m_{f_{M_i} \to X_i}(x_i)}$.

If the noise precision is to be estimated, λ is replaced by $\hat{\lambda}^t$ in the algorithms and is updated using (10) following Steps 4 and 8 in **Algorithm 1** and Step 4 in **Algorithm 2**.

IV. BP AND GAMP METHOD

We briefly present the application of the GAMP algorithm to the SC-FDE system. As for the BP-MF method, the factor graph shown in Fig. 1 is also divided into two parts, a BP part and a GAMP part. GAMP [9] is implemented for equalization and BP is used for demodulation and decoding. The messages from the BP part $\{m^t_{f_{M_i} \to X_i}(x_i)\}$ are used to compute the means $\{\mu^t_{X_i}\}$ and variances $\{\nu^t_{X_i}\}$ of the beliefs $\{b(x_i)\}$. The extrinsic messages from nodes $\{X_i\}$ to nodes $\{f_{M_i}\}$, $\{m^t_{X_i \to f_{M_i}}(x_i) = \mathcal{CN}(x_i; \mu^t_{r_i}, \nu^t_{r_i})\}$, are used for soft demodulation. The BP-GAMP algorithm, proposed in [11], is described in **Algorithm 3**.

Algorithm 3 BP-GAMP Receiver

1:   **for all** i: initialize $\mu^0_{X_i}, \nu^0_{X_i}$.

2:   $\boldsymbol{\mu}^0_S \leftarrow \boldsymbol{0}; \boldsymbol{\mu}_Z = \boldsymbol{y}./\boldsymbol{h}; \boldsymbol{\nu}_Z = 1./(\lambda \boldsymbol{h} \odot \boldsymbol{h}^*)$

3:   **for** $t = 1 \to$ Iteration **do**

4:       $\boldsymbol{\nu}^t_P \leftarrow \boldsymbol{1} \sum_{i=1}^{N} \nu^{t-1}_{X_i}/N$

5:       $\boldsymbol{\mu}^t_P \leftarrow \boldsymbol{F}\boldsymbol{\mu}^{t-1}_X - \boldsymbol{\mu}^{t-1}_S \odot \boldsymbol{\nu}^t_P$,

6:       $\boldsymbol{\nu}^t_S \leftarrow 1./(\boldsymbol{\nu}_Z + \boldsymbol{\nu}^t_P)$

7:       $\boldsymbol{\mu}^t_S \leftarrow (\boldsymbol{\mu}_Z - \boldsymbol{\mu}^t_P) \odot \boldsymbol{\nu}^t_S$

8:       $\boldsymbol{\nu}^t_R \leftarrow \boldsymbol{1} N/(\sum_{a=1}^{N} \nu^t_{S_a})$

9:       $\boldsymbol{\mu}^t_R \leftarrow \boldsymbol{\mu}^{t-1}_X + \boldsymbol{\nu}^t_R \odot (\boldsymbol{F}^H \boldsymbol{\mu}^t_S)$

10:      **for all** i: $\mathcal{CN}(x_i; \mu^t_{R_i}, \nu^t_{R_i}) \to$ BP part.

11:      **for all** i: $m^t_{f_{M_i} \to X_i}(x_i) \leftarrow$ BP part.

12:      **for all** i: $\mu^t_{X_i} \leftarrow \langle x_i \rangle_{\mathcal{CN}(x_i; \mu^t_{R_i}, \nu^t_{R_i}) m^t_{f_{M_i} \to X_i}(x_i)}$

13:      **for all** i: $\nu^t_{X_i} \leftarrow \text{var}[x_i]_{\mathcal{CN}(x_i; \mu^t_{R_i}, \nu^t_{R_i}) m^t_{f_{M_i} \to X_i}(x_i)}$

14: **end for** t

where $\boldsymbol{\mu}^t_X = [\mu^t_{X_1}, \ldots, \mu^t_{X_N}]^T$, $\odot$ and $./$ stand for component-wise product and division, respectively, and $\nu^t_{S_a}$ denotes the ath entry of $\boldsymbol{\nu}^t_S$.

V. SIMULATION RESULTS

We consider an SC-FDE system with $N = 256$ data symbols per block and a bandwidth of $W = N * 15$ KHz. A block of data symbols is obtained from a sequence of information bits encoded using a rate $R = 1/3$ convolutional code with generator polynomials $(133, 171, 165)_8$, or a rate $R = 1/2$ code with $(5, 7)_8$. Random interleaving and QPSK or 16QAM modulation are subsequently applied. The realizations of the channel transfer function are generated using the 3GPP ETU channel model and their samples $\boldsymbol{h}$ are assumed to be known at the receiver side. We assess the performance of receivers implementing three different algorithms: BP-MF with sequential scheduling (BP-MF-s), BP-MF with parallel scheduling (BP-MF-p), and BP-GAMP. For the BP-MF receivers, we allow two different variants: one in which the noise precision (NP) λ is assumed to be known (Known NP) and one in which it is re-estimated at every iteration of the algorithms (Unknown NP). To include an ideal reference,
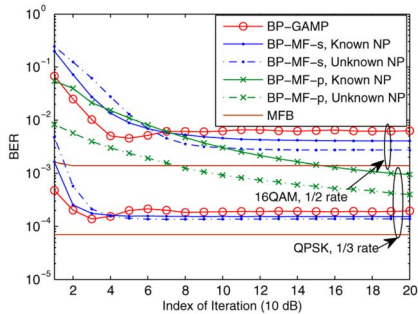
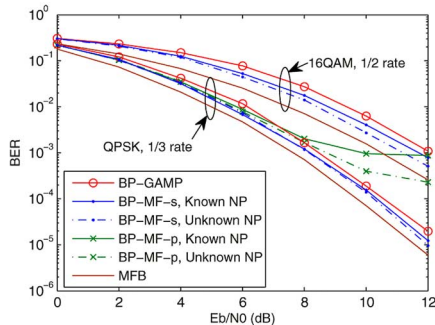Fig. 2. BER performance of the considered receivers versus iteration index for an Eb/N0 of 10 dB.

Fig. 3. BER performance of the considered receivers versus Eb/N0.

the matched-filter bound (MFB) is also evaluated. The MFB is the performance of a receiver which, when detecting a symbol in an SC-FDE block, has perfect knowledge of every other symbol in the block and the noise precision.

In Fig. 2, the BER of the receivers operating at a SNR of 10 dB is depicted as a function of the iteration index. Two different modulation schemes and coding rates have been selected: a low-rate (R = 1/3) system using QPSK modulation, and a high-rate (R = 1/2) system employing 16QAM. For the BP-MF receiver, we observe that convergence is dramatically improved by using the sequential schedule as compared to the parallel schedule. The latter requires more than 30 iterations to converge in the low-rate case.[1] The reason for this is that, with the serial schedule, the estimates of the data symbols that have already been obtained in the course of the tth iteration are immediately used to estimate those data symbols which have not yet been estimated during iteration t. Conversely, with the parallel schedule such estimates are not used for equalization until the $(t + 1)$th iteration. The BP-GAMP algorithm, for its part, exhibits an erratic BER behavior in the first iterations, before stabilizing to BER values slightly higher than those achieved by the BP-MF-s receiver.

In Fig. 3, the BER performance of the receivers is shown over a wide range of SNR values, with all receivers running 20 iterations of their respective algorithms. As already observed in Fig. 2, the BP-MF-s receiver performs best of all receivers, with gains of 0.5 dB and 1 dB with respect to the BP-GAMP receiver for the low- and high-rate systems, respectively. The BP-MF-p receiver achieves a performance similar to that of its sequential counterpart in the lowest SNR range, but its convergence is too slow to be used at larger SNR values.

Interestingly, including the estimation of the noise precision in the BP-MF-s receiver has two effects, as seen from Figs. 2 and 3: on the one hand, it slightly slows down the convergence

---

[1]This effect is even more pronounced for the high-rate case. Results have been omitted in the plot.

speed of the algorithm; on the other hand, the performance obtained after convergence is slightly better than that of the receiver which has knowledge of the true noise precision. As the variance of the estimates of the data symbols are integrated in the noise precision estimates, the algorithm including the noise precision estimation exhibits a more robust behaviour, at the expense of a slightly lower convergence speed.

In terms of computational complexity, we point out that all three receivers differ only in the equalization part. For this part, the BP-MF-p and BP-GAMP receivers have similar complexity, in the order of $\mathcal{O}(N \log_2 N)$ complex operations, as FFT processing can be used due to the passing of messages being parallel. The FFT cannot be used when messages are passed sequentially, which increases the complexity of the BP-MF-s equalization part to $\mathcal{O}(N^2)$ per SC-FDE block.

VI. CONCLUSION

Based on the BP-MF inference framework, we have developed parallel and sequential message-passing receivers for joint equalization and decoding in an SC-FDE system and compared their performance to that of an analogous receiver using GAMP for equalization.

Our numerical assessment shows that, for the considered SC-FDE system, the receiver using the BP-MF framework with sequential message-passing schedule is superior, in terms of performance, to its parallel counterpart and the receiver using GAMP. This performance improvement comes at the expense of an increase in computational complexity. Additionally, our results show that embedding the estimation of the noise precision parameter in the iterative algorithm improves the receiver's performance even when the true value of this parameter is known beforehand.

REFERENCES

[1] D. Falconer, S. Ariyavisitakul, A. Benyamin-Seeyar, and B. Eidson, "Frequency domain equalization for single-carrier broadband wireless systems," *IEEE Commun. Mag.*, vol. 40, no. 4, pp. 58–66, Apr. 2002.

[2] E. Dahlman, S. Parkvall, J. Sköld, and P. Beming, *3G Evolution: HSPA and LTE for Mobile Broadband*, 2nd ed. ed. New York, NY, USA: Academic, 2008.

[3] F. Kschischang, B. Frey, and H.-A. Loeliger, "Factor graphs and the sum-product algorithm," *IEEE Trans. Inf. Theory*, vol. 47, no. 2, pp. 498–519, Feb. 2001.

[4] G. Parisi, *Statistical Field Theory*. New York, NY, USA: Perseus, 1988.

[5] J. Winn and C. Bishop, "Variational message passing," *J. Machine Learn. Res.*, vol. 6, pp. 661–694, 2005.

[6] E. Riegler, G. E. Kirkelund, C. N. Manchón, M.-A. Badiu, and B. H. Fleury, "Merging belief propagation and the mean field approximation: A free energy approach," *IEEE Trans. Inf. Theory*, vol. 59, no. 1, pp. 588–602, Jan. 2013.

[7] C. N. Manchón, G. E. Kirkelund, E. Riegler, L. P. B. Christensen, and B. H. Fleury, "Receiver architectures for MIMO-OFDM based on a combined VMP-SP algorithm," 2011, arXiv:1111.5848 [stat.ML]..

[8] M. Bayati and A. Montanari, "The dynamics of message passing on dense graphs, with applications to compressed sensing," *IEEE Trans. Inf. Theory*, vol. 57, no. 2, pp. 764–785, Feb. 2011.

[9] S. Rangan, "Generalized approximate message passing for estimation with random linear mixing," in *Proc. IEEE Int. Symp. Inform. Theory (ISIT 2011)*, Aug. 2011, pp. 2168–2172.

[10] P. Schniter, "A message-passing receiver for BICM-OFDM over unknown clustered-sparse channels," *IEEE J. Sel. Topics Signal Process.*, vol. 5, no. 8, pp. 1462–1474, Dec. 2011.

[11] Q. Guo, D. Huang, S. Nordholm, J. Xi, and Y. Yu, "Iterative frequency domain equalization with generalized approximate message passing," *IEEE Signal Process. Lett.*, vol. 20, no. 6, pp. 559–562, Jun. 2013.

[12] M. Nassar, P. Schniter, and B. Evans, "A factor graph approach to joint ofdm channel estimation and decoding in impulsive noise environments," *IEEE Trans. Signal Process.*, vol. 62, no. 6, pp. 1576–1589, Mar. 2014.